

Fine YAG:Ce³⁺ nanoparticles synthesised by supercritical hydrothermal reaction

Shibing Qian, Yongqing Ma, Fenlian Zan, Dan Zou, Zhenxiang Dai, Ganhong Zheng, Guang Li

Anhui Key Laboratory of Information Materials and Devices, School of Physics and Materials Science, Anhui University, Hefei 230039, People's Republic of China

E-mail: yqma@ahu.edu.cn

Published in Micro & Nano Letters; Received on 3rd December 2012; Revised on 3rd February 2013; Accepted on 6th February 2013

Yttrium aluminium garnet (YAG):Ce³⁺ nanoparticles have been synthesised by the supercritical hydrothermal method at 390 °C in a series of reaction times of 2, 4, 6, 8, 10 and 12 h, respectively, and characterised by X-ray diffraction, a scanning electron microscope, (high resolution) transmission electron microscopy and several measurements of fluorescence properties. The single-phase YAG:Ce³⁺ can be obtained at much lower temperature (390 °C) by means of the supercritical hydrothermal method with inexpensive raw materials and simple processing conditions than by the conventional solid-state method and other wet-chemical methods. The YAG:Ce³⁺ phosphors synthesised by the supercritical hydrothermal method exhibit more uniform size distribution and stronger emission, compared with those synthesised at the 360 °C below the supercritical point of water. The reaction time also influences the luminescent properties, and the related mechanism is discussed.

1. Introduction: Recently, compared with the incandescence of fluorescent lamps, the white light-emitting diode (WLED) has been extensively investigated because of its advantages such as high luminous efficiency, high reliability, long lifetime, low-energy consumption, safety and its environment-friendly characteristics, and will become the fourth generation lighting sources to replace incandescent and fluorescent lamps [1–3]. Yttrium aluminium garnet (YAG):Ce³⁺ phosphors have been found to be suitable for absorbing the blue LED radiation and down-convert a very broadband yellow emission, which can be used as one common approach to producing white light with a gallium nitride-based blue LED.

The most common process to produce YAG:Ce³⁺ phosphor is traditional solid-state reaction which usually needs a high temperature of 1600 °C with flux, such as B₂O₃ and BaF₂, which generally introduces additional impurities and defects [4]. Additionally, the traditional process normally leads to large grain sizes and irregular shape, which greatly deteriorate the luminescent properties. YAG and YAG:Ce³⁺ particles have been also produced using the co-precipitation process [5, 6], the glycothermal method [7–11], combustion synthesis [12], spray-pyrolysis [13, 14] and the solvothermal method etc. Among the above wet-chemical methods, it usually needs subsequent treatment or a higher reaction temperature to obtain the single-phase YAG. For example, Y₃Al₅O₁₂:Ce³⁺ nanophosphor powders synthesised via a solvothermal method at 220 °C for 2 h needs post-annealing at 1150 W using a single-mode cavity of 2.45 GHz microwaves [15]. Li and Shen [16] have prepared single-phase YAG with expensive raw materials (aluminium isopropoxide, yttrium acetate, cerium acetate and gadolinium acetate) by placing the precursor solution in an autoclave and heating to 600 °C with continuous stirring at 500 rpm. Recently, supercritical water has been successfully applied in synthesising functional inorganic materials as an excellent media [17–19]. Zheng *et al.* [20] have prepared mono-dispersed YAG and rare earth-doped YAG nanophosphors with spherical or polyhedron morphology and the size distribution from 100 to 500 nm. J.-H. In *et al.* [21] have prepared single-phase YAG phosphor by directly feeding potassium hydroxide solution and metal salt solution to supercritical water (400 °C and 280 bar) with complicated apparatus and processing conditions.

It is well known that the properties of water, such as its viscosity, diffusivity, density, static dielectric constant and so on, are changed with slight variations of temperature and pressure at its near critical point (374 °C). Furthermore, the supercritical water is a

homogeneous reaction media with unique chemical and physical properties. In this study, we have prepared the fine nanophosphors Y_{2.95}Ce_{0.05}Al₅O₁₂ with inexpensive raw materials by the supercritical hydrothermal method (390 °C and 24.7 MPa) with simple processing conditions. By changing the reaction time, we aim to obtain the single-phase YAG:Ce³⁺ at low temperature with good dispersion and uniform size and to study the effects of the reaction time on the luminescent properties of YAG:Ce³⁺ nanoparticles.

2. Experimental work: The nanophosphors Y_{2.95}Ce_{0.05}Al₅O₁₂ were prepared by a supercritical hydrothermal method. The reactants include Ce(NO₃)₃·6H₂O (99.99%), Al(NO₃)₃·9H₂O (99%), Y(NO₃)₃·6H₂O (99.99%) and NH₄HCO₃.

At first, an appropriate amount of Y(NO₃)₃·6H₂O, Ce(NO₃)₃·6H₂O and Al(NO₃)₃·9H₂O was dissolved in distilled water with the mole ratios of the Y³⁺, Ce³⁺ and Al³⁺ being 2.95:0.05:5 to form the mixed solution. The ammonium hydrogen carbonate (AHC) solution was prepared by adding NH₄HCO₃ into 200 ml of distilled water. Then, the precursor precipitate was prepared by adding dropwise the mixed solution into the above AHC solution under vigorous agitation at room temperature. After being aged for 24 h, the precipitate was repeatedly washed with distilled water to remove the residual nitric and ammonia ions. At last, precursor precipitate was dispersed in 250 ml distilled water and transferred into a 1000 ml autoclave (Parr 4577, USA). The hydrothermal reaction was kept at 390 °C with the pressure of 24.7 MPa and the stirring speed of 150 rpm for different reaction times (denoted by *t_r*, below) of 2, 4, 6, 8, 10 and 12 h, respectively. After cooling naturally to room temperature, the autoclave was opened, and the products were washed with distilled water and dried at 60 °C for further study.

The crystal structure of the phosphor powders was characterised by X-ray diffraction (XRD) analysis, using an X-ray diffractometer (DX-2000 SSC) with Cu K α irradiation ($\lambda = 1.5406$ Å) with an operating voltage of 36 kV and operating current of 25 mA. The activation and emission spectra were measured on an FL fluorescence spectrophotometer (F-4500) with the same sample mass. The surface morphologies were observed using a scanning electron microscope (SEM, S-4800, Hitachi). (High-resolution) transmission electron microscopy ((HR) TEM) (JEOL JEM-2100) was used to observe the lattice fringe and to obtain the selected area electron diffraction (SAED) pattern. The decay curve of transitions was measured on an EasyLife L with FluoreScan version 3.0. All the measurements were carried out at room temperature.

3. Results and discussion

3.1. Crystal structures of the nanophosphors $\text{Y}_3\text{Al}_5\text{O}_{12}:\text{Ce}^{3+}$: The XRD results indicate that the diffraction peak positions and the relative intensities of all the prepared nanophosphors are well matched with those of the JCPDS (No. 88–2048) pattern of $\text{Y}_3\text{Al}_5\text{O}_{12}$. Figs. 1a–c representatively show the XRD patterns of the nanophosphors $\text{Y}_3\text{Al}_5\text{O}_{12}:\text{Ce}$ with $t_r = 2, 6$ and 10 h, which indicate that the nanophosphors are single phase with no detectable secondary phases and have a cubic structure with the space group Ia-3d. These results indicate that the single-phase YAG:Ce can be synthesised by the supercritical hydrothermal method at a much lower temperature (390°C) than that ($\sim 1600^\circ\text{C}$) by the conventional solid-state method and by a simple processing conditions without the subsequent treatment. The crystallite size of nanophosphors $\text{Y}_{2.95}\text{Ce}_{0.05}\text{Al}_5\text{O}_{12}$ calculated by MDI Jade 5.0 software are shown in Fig. 2a, exhibiting an irregular variation with increasing t_r , which may result from the complex process for the crystal nucleating and growing during the supercritical hydrothermal reaction. The lattice parameters of cubic YAG were calculated according to $\sin^2\theta = (\lambda^2/4a^2)(H^2 + K^2 + L^2)$, where a is the lattice parameter, θ diffraction angle, λ the wavelength of Cu $K\alpha$ irradiation, and (HKL) the crystal plane index. The obtained results are given in Fig. 2b, which are consistent with the previous report [22].

3.2. Microstructural analyses of the nanophosphors $\text{Y}_3\text{Al}_5\text{O}_{12}:\text{Ce}^{3+}$: Figs. 3a–f show the SEM images of YAG:Ce³⁺ nanophosphors with $t_r = 2, 4, 6, 8, 10$ and 12 h, respectively. As a contrast, Figs. 4a and b show the SEM images of YAG:Ce³⁺ prepared at 360°C (below the supercritical temperature of water) with $t_r = 6$ and 10 h keeping the other processing conditions the same. It can be seen that YAG:Ce³⁺ prepared at 390°C exhibits the more uniform size.

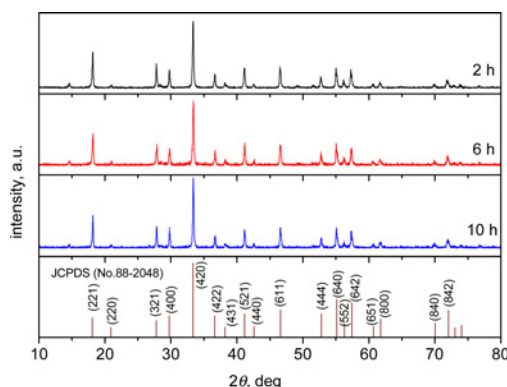


Figure 1 XRD patterns of the nanophosphors $\text{Y}_3\text{Al}_5\text{O}_{12}:\text{Ce}$ with $t_r = 2, 6$ and 10 h and the standard JCPDS (No. 88–2048) pattern

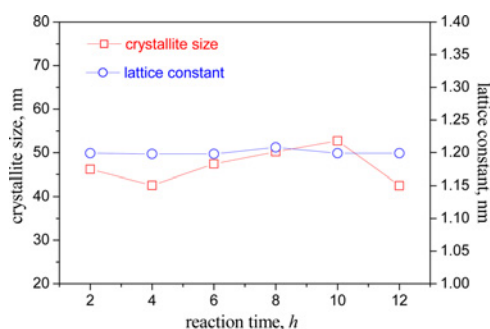


Figure 2 Crystallite size and the lattice parameter of nanophosphors $\text{Y}_{2.95}\text{Ce}_{0.05}\text{Al}_5\text{O}_{12}$ with $t_r = 2, 4, 6, 8, 10$ and 12 h

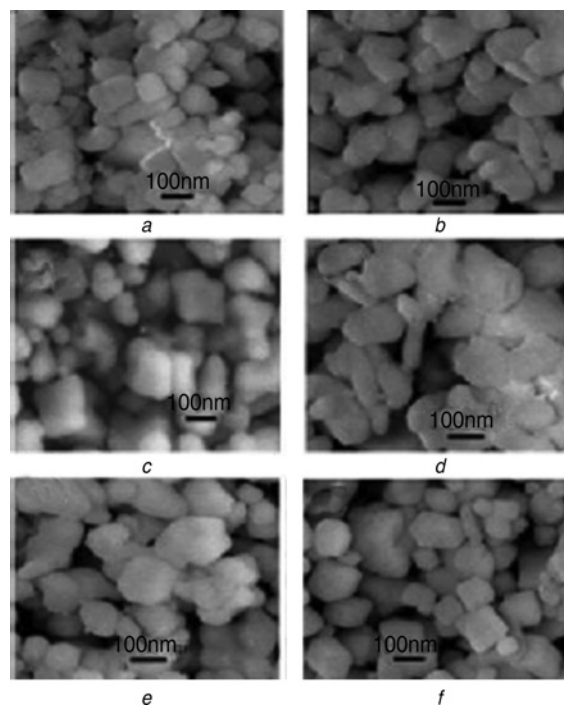


Figure 3 SEM images of YAG:Ce³⁺ nanophosphors with $t_r = 2, 4, 6, 8, 10$ and 12 h

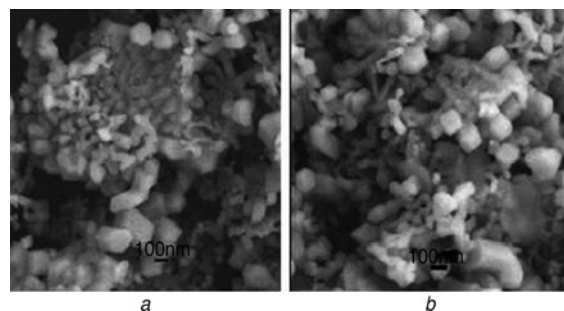


Figure 4 SEM images of YAG:Ce³⁺ prepared at 360°C (below the supercritical temperature of water) with $t_r = 6$ and 10 h

Figs. 5a–f show the size distribution analysis by Gaussian fit of the histogram drawn from the SEM images in Fig. 3. The average size of most particles is about 94, 104, 109, 116, 132 and 139 nm in the samples prepared with $t_r = 2, 4, 6, 8, 10$ and 12 h, respectively, indicating that the particle size increases with increasing t_r .

To investigate the microstructure of the nanophosphors further, Fig. 6a representatively shows the TEM image for the sample with $t_r = 6$ h. The cubic- and spherical-like particles co-exist in the sample. Figs. 6b and c show the HRTEM lattice fringes and SAED results photographed from the area labelled by the square in Fig. 6a. As shown in Fig. 6b, the interfringe distance of 0.498 nm corresponds to the (211) crystalline plane of YAG. As shown in Fig. 6c, the distinct diffraction spots can be indexed to diffraction of (211), (220), (422) and (431) planes. Both the HRTEM and the SAED results indicate that the sample prepared by the supercritical hydrothermal method is characterised by high crystallinity and a perfect crystal structure.

3.3. Photoluminescence properties of the nanophosphors $\text{Y}_3\text{Al}_5\text{O}_{12}:\text{Ce}^{3+}$: Fig. 7 shows the activation spectra of the nanophosphors $\text{Y}_3\text{Al}_5\text{O}_{12}:\text{Ce}^{3+}$ with $t_r = 2, 4, 6, 8, 10$ and 12 h for monitoring the most intense emission of Ce³⁺ at $\lambda_{em} = 540$ nm. All the activation spectra show the similar spectral features

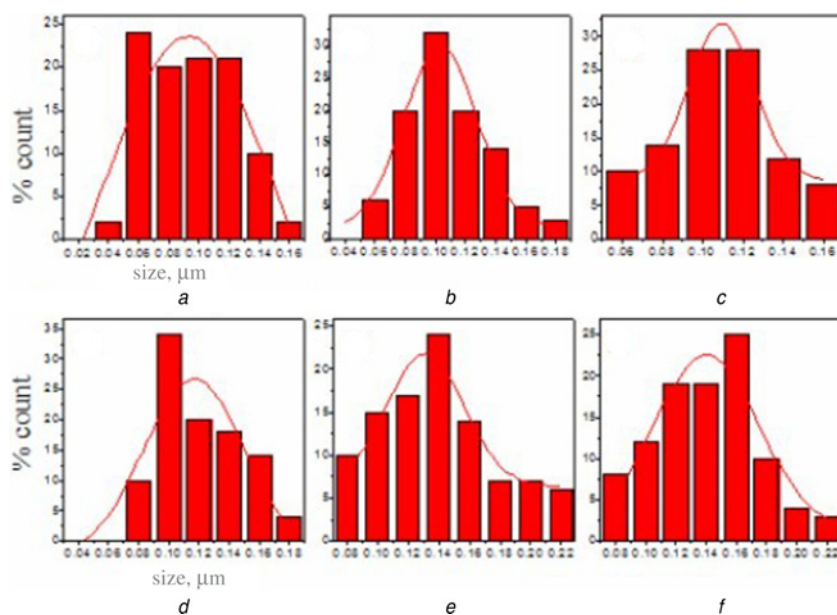


Figure 5 Size distribution analysis by Gaussian fit of the histogram drawn from SEM images in Fig. 3 with $t_r = 2, 4, 6, 8, 10$ and 12 h

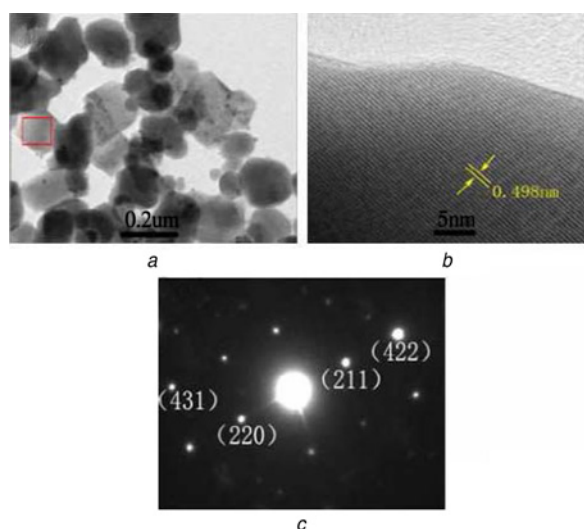


Figure 6 TEM image, the HRTEM lattice fringes and SAED of YAG:Ce³⁺ nanophosphors with $t_r = 6$ h

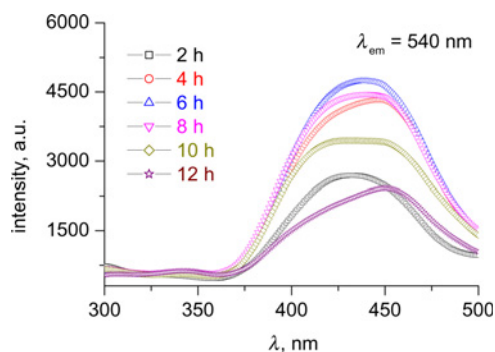


Figure 7 Activation spectra of the nanophosphors Y₃Al₅O₁₂:Ce³⁺ with $t_r = 2, 4, 6, 8, 10$ and 12 h for monitoring the most intense emission of Ce³⁺ at $\lambda_{em} = 540$ nm

except for the different intensity. A weak band peaks around 340 nm, and the other broad and strong band ranges from 360 to 500 nm, which can be assigned to the transitions of $^2F_{5/2} \rightarrow ^5D$ and $^2F_{7/2} \rightarrow ^5D$ of Ce³⁺, respectively, in the 4f¹ electron configuration of Ce³⁺. The sample with $t_r = 6$ h shows the most intense excitation. Such a broad and strong excitation band matches well with the blue InGaN LED excitation because of the emission wavelength of InGaN LED chips located in the range of 450–480 nm.

Fig. 8 shows the emission spectra of nanophosphors Y₃Al₅O₁₂:Ce³⁺ with $t_r = 2, 4, 6, 8, 10$ and 12 h with the activation wavelength of 440 nm ($\lambda_{ex} = 440$ nm). The emission spectra exhibit a broad-band in the wavelength range of 470–650 nm with the emission peak locating around 540 nm, originating from transitions from the 5d states to the 4f states. Fig. 9 shows the dependence of the most emission intensity of Ce³⁺ at 540 nm on the reaction time from $t_r = 2$ to 12 h. With increasing t_r , the emission intensity increases, experiencing a maximum at $t_r = 6$ h, and then decreases with the reaction time. The variation of the emission intensity with the reaction time can be suggested to result from the competition between the crystallite size and the particle size. With increasing the reaction time, the sample crystallises better which can be evidenced by the results in Fig. 2a because the crystallite size increases with the reaction time increasing from 4 to 10 h. The

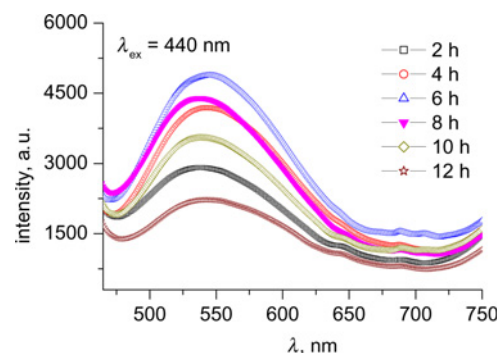


Figure 8 Emission spectra of nanophosphors Y₃Al₅O₁₂:Ce³⁺ with $t_r = 2, 4, 6, 8, 10$ and 12 h with the activation wavelength of 440 nm

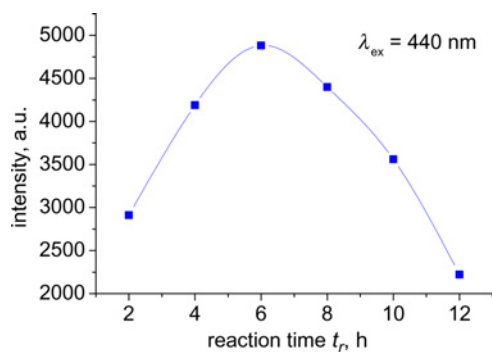


Figure 9 Dependence of the most emission intensity of Ce^{3+} at 540 nm on the reaction time from $t_r = 2$ to $t_r = 12$ h

better crystallisation will lead to the decrease of defects in the sample and the reduction of the non-radiation recombination probability, consequently resulting in the enhancement of the emission intensity. Further increasing the reaction time will enlarge the particle size as shown in Fig. 5, leading to the smaller cross-section for absorbing the excitation light [23], consequently resulting in the decrease of the emission intensity. Additionally, as a contrast, Fig. 10 shows the emission spectra of $\text{YAG}:\text{Ce}^{3+}$ prepared at 390 and 360 °C (below the supercritical temperature of water) with $t_r = 6$ h keeping the other processing conditions the same. The emission intensity of $\text{YAG}:\text{Ce}^{3+}$ prepared at 390 °C obviously exceeds that prepared at 360 °C, which may result from the better crystallisation and more uniform size distribution.

Fig. 11 shows the decay curve of transitions from the 5d states to the 4f states of Ce^{3+} under an excitation of 440 nm. All the decay

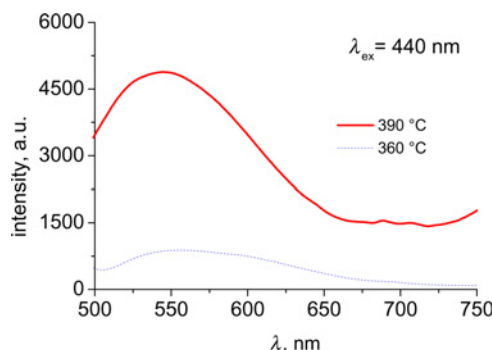


Figure 10 Emission spectra of $\text{YAG}:\text{Ce}^{3+}$ prepared at 390 and 360 °C (below the supercritical temperature of water) with $t_r = 6$ h

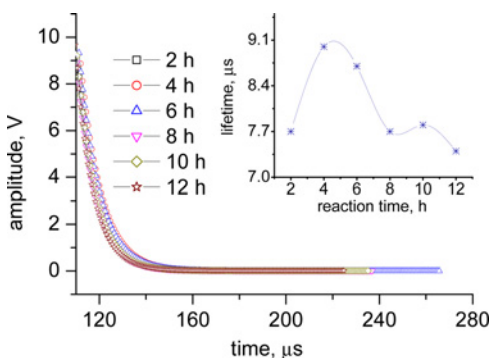


Figure 11 Decay curve of transitions from the 5d states to the 4f states of Ce^{3+} under an excitation of 440 nm

curves present a single-exponential decay behaviour, which can be represented by $I = I_0 \exp(-t/\tau)$, where I and I_0 are the luminescence intensities at time t and 0 and the t radiative decay time [24], which indicates that the coordination environment of the rare earth ions is homogeneous in the $\text{YAG}:\text{Ce}^{3+}$ samples [25]. With increasing the reaction time, the luminescence life first increases and then decreases after $t_r > 4$ h. As reported before [26], the better crystallisation will lead to increase of the decay lifetime because of the reduction in the non-radiative process arising from crystal defects. However, it is not the case for all samples. Perhaps, for the longer reaction time, there may appear Ce^{4+} in the sample because of oxidation, which enhances the non-radiative transition of 4f electrons between Ce^{3+} and Ce^{4+} , leading to the shorter lifetime. Furthermore, the Ce^{4+} ions with 4f⁰ electronic configuration cannot emit light which may be another reason for the decrease of emission intensity for the sample with longer reaction time.

4. Conclusions: We have synthesised the nanophosphors $\text{YAG}:\text{Ce}^{3+}$ (5 % mol.) with different reaction times ($t_r = 2, 4, 6, 8, 10$ and 12 h) by the supercritical hydrothermal method (390 °C and 24.7 MPa) and investigated their structure, morphology, size distribution and luminescent properties. We can obtain the single-phase $\text{YAG}:\text{Ce}^{3+}$ at much lower temperature (390 °C) by means of the supercritical hydrothermal method with the inexpensive raw materials and simple processing conditions than by the conventional solid-state method and the other wet-chemical methods. The reaction time plays an important role in the crystallisation, particle size and luminescent properties. The results of XRD and SEM illustrate that the crystallisation becomes roughly better and average particle size becomes larger with increasing the reaction time, and the sample prepared above the supercritical point of water shows the more uniform size distribution than that prepared below the supercritical point of water. The photoluminescence spectra reveal that the sample with the reaction time of 6 h has the most intense emission which results from the competition between the crystallite size and the particle size. The luminescent decay results suggest that the longer reaction time may induce a Ce^{4+} with 4f⁰ electron configuration which cannot emit light, and it may be another reason for the decrease of emission intensity with increasing the reaction time. Furthermore, the sample synthesised by the supercritical hydrothermal method exhibits stronger emission than that synthesised at 360 °C below supercritical point of water, which may result from the better crystallisation and more uniform size distribution of particles for the former sample.

5. Acknowledgments: This work was financially supported by the National Science Foundation of China under grant numbers 11174004, 10804110 and 11204001; also by the Anhui Province Natural Science Foundation (grant number 1208085QA07), and by the Anhui University Scientific Research Fund numbers 06060283, 2009QN006A and 32030028, and the ‘211 Project’ of Anhui University.

6 References

- [1] Schubert E.F., Kim J.K.: ‘Solid-state light sources getting smart’, *Science*, 2005, **308**, pp. 1274–1278
- [2] Hoppe H.A.: ‘Recent developments in the field of inorganic phosphors’, *Angew. Chem., Int. Ed.*, 2009, **48**, pp. 3572–3582
- [3] Li P.L., Wang Z.J., Yang Z.P., Guo Q.L., Fu G.S.: ‘Luminescent characteristics of $\text{LiSrBO}_3:\text{M}$ ($\text{M} = \text{Eu}^{3+}, \text{Sm}^{3+}, \text{Tb}^{3+}, \text{Ce}^{3+}, \text{Dy}^{3+}$) phosphor for white light-emitting diode’, *Mater. Res. Bull.*, 2009, **44**, pp. 2068–2071
- [4] Hong S., Fu Z., Zhang J., Zhang S.: ‘Spectral properties of rare-earth ions in nanocrystalline $\text{YAG}:\text{Re}$ ($\text{Re} = \text{Ce}^{3+}, \text{Pr}^{3+}, \text{Tb}^{3+}$)’, *J. Lumin.*, 2006, **118**, pp. 179–185
- [5] Jung K.Y., Kang Y.C.: ‘Luminescence comparison of $\text{YAG}:\text{Ce}$ phosphors prepared by microwave heating and precipitation methods’, *Physica B*, 2010, **405**, pp. 1615–1618

- [6] Li J., Chen F., Liu W.B., *ET AL.*: 'Co-precipitation synthesis route to yttrium aluminum garnet (YAG) transparent ceramics', *J. Eur. Ceram. Soc.*, 2012, **32**, pp. 2971–2979
- [7] Jia N.T., Zhang X.D., He W., Hu W.J., Meng X.P., Du Y.: 'Property of YAG:Ce phosphors powder prepared by mixed solvothermal method', *J. Alloys Compd.*, 2011, **509**, pp. 1848–1853
- [8] Rai P., Song M.-K., Song H.-M., *ET AL.*: 'Synthesis, growth mechanism and photoluminescence of monodispersed cubic shape Ce doped YAG nanophosphor', *Ceram. Int.*, 2012, **38**, pp. 235–242
- [9] Wu Z.G., Zhang X.D., He W., Du Y.W., Jia N.T., Xu G.G.: 'Preparation of YAG:Ce spheroidal phase-pure particles by solvo-thermal method and their photoluminescence', *J. Alloys Compd.*, 2009, **468**, pp. 571–574
- [10] Nyman M., Shea-Rohwer L.E., Martin J.E., Provencio P.: 'Nano-YAG:Ce mechanisms of growth and epoxy-encapsulation', *Chem. Mater.*, 2009, **21**, pp. 1536–1542
- [11] Su L.T., Tok A.I.Y., Zhao Y., Ng N., Boey F.Y.C.: 'Synthesis and electron-phonon interactions of Ce³⁺-doped YAG nanoparticles', *J. Phys. Chem. C*, 2009, **115**, pp. 5974–5979
- [12] Yang Z.P., Li X., Yang Y., Li X.M.: 'The influence of different conditions on the luminescent properties of YAG:Ce phosphor formed by combustion', *J. Lumin.*, 2007, **122**, p. 707
- [13] Zhou Y.H., Lin J., Yu M., Han S.M., Wang S.B., Zhang H.J.: 'Morphology control and luminescence properties of YAG:Eu phosphors prepared by spray pyrolysis', *Mater. Res. Bull.*, 2003, **38**, pp. 1289–1299
- [14] Lee S.H., Koo H.Y., Lee S.M., Kang Y.C.: 'Characteristics of Y₃Al₅O₁₂:Ce phosphor powders prepared by spray pyrolysis from ethylenediaminetetraacetic acid solution', *Ceram. Int.*, 2010, **36**, pp. 611–615
- [15] Bhaskar A., Chang H.-Y., Chang T.-H., Cheng S.-Y.: 'Microwave annealing of YAG:Ce nanophosphors', *Mater. Lett.*, 2012, **78**, pp. 124–126
- [16] Li K., Shen C.Y.: 'White LED based on nano-YAG:Ce³⁺/YAG:Ce³⁺, Gd³⁺ hybrid phosphors', *Optik*, 2012, **123**, pp. 621–623
- [17] Kempaiah Devaraju M., Yin S., Sato T.: 'Eu³⁺:Y₂O₃ microspheres and microcubes: a supercritical synthesis and characterization', *Inorg. Chem.*, 2011, **50**, pp. 4698–4704
- [18] Ohara S., Mousavand T., Umetsu M., *ET AL.*: 'Hydrothermal synthesis of fine zinc oxide particles under supercritical conditions', *Solid State Ion.*, 2004, **172**, pp. 261–264
- [19] Devaraju M.K., Yin S., Sato T.: 'Solvothermal synthesis controlled morphology and optical properties of Y₂O₃:Eu³⁺ nanocrystals', *J. Cryst. Growth*, 2009, **311**, pp. 580–584
- [20] Zheng Q.X., Li B., Zhang H.D., Zheng J.J., Jiang M.H., Tao X.T.: 'Fabrication of YAG mono-dispersed particles with a novel combination method employing supercritical water process', *J. Supercrit. Fluids*, 2009, **50**, pp. 77–81
- [21] In J.-H., Lee H.-C., Yoon M.-J., Lee K.-K., Lee J.-W., Lee C.-H.: 'Synthesis of nano-sized YAG:Eu³⁺ phosphor in continuous supercritical water system', *J. Supercrit. Fluids*, 2007, **40**, pp. 389–396
- [22] Huang Z.C., Feng J., Pan W.: 'First-principles calculations of structural and thermodynamic properties of Y₃Al₅O₁₂', *Solid State Commun.*, 2011, **151**, pp. 1559–1563
- [23] Yu Y.Q., Zhou S.H., Zhang S.Y.: 'Luminescence of the compounds Y_{0.5–x}Li_{1.5}VO₄:(Dy³⁺, Eu³⁺)_x', *J. Alloys Compd.*, 2003, **351**, p. 84
- [24] Chang Y.-S., Huang F.-M., Tsai Y.-Y., Teoh L.-G.: 'Synthesis and photoluminescent properties of YVO₄:Eu³⁺ nano-crystal phosphor prepared by Pechini process', *J. Lumin.*, 2009, **129**, pp. 1181–1185
- [25] Yu M., Lin J., Wang Z., *ET AL.*: 'Fabrication, patterning, and optical properties of nanocrystalline YVO₄:A (A = Eu³⁺, Dy³⁺, Sm³⁺, Er³⁺) phosphor films via sol-gel soft lithography', *Chem. Mater.*, 2002, **14**, pp. 2224–2231
- [26] Shanta Singh N., Ningthoujam R.S., Yaiphaba N., Dorendrajit Singh S., Vatsa R.K.: 'Lifetime and quantum yield studies of Dy³⁺ doped GdVO₄ nanoparticles: concentration and annealing effect', *J. Appl. Phys.*, 2009, **105**, p. 64303